

Tunneling dynamics of a hydroxyl group adsorbed on Cu(110)

T. Kumagai, M. Kaizu, and H. Okuyama*

Department of Chemistry, Graduate School of Science, Kyoto University, Kyoto 606-8502, Japan

S. Hatta and T. Aruga

Department of Chemistry, Graduate School of Science, Kyoto University, Kyoto 606-8502, Japan and JST CREST, Saitama 332-0012, Japan

I. Hamada and Y. Morikawa

The Institute of Scientific and Industrial Research, Osaka University, 8-1 Mihogaoka, Ibaraki, Osaka 567-0047, Japan

(Received 26 August 2008; revised manuscript received 14 December 2008; published 30 January 2009)

Dynamics of a hydroxyl (OH) group and its dimer adsorbed on Cu(110) is investigated at 6 K with a scanning tunneling microscope (STM). For the monomer, the inclined OH axis switches back and forth between the two equivalent orientations via hydrogen-atom tunneling. The motion is enhanced by tunneling electron that excites the OH bending mode that directly correlates with the reaction coordinate. The inelastic electron-tunneling spectra exhibit either peak or dip, depending on the position of the STM tip over the molecule. The switch motion is quenched for the hydroxyl dimer since it is stabilized by hydrogen-bond formation, whereas it is induced by inelastic excitation of the OH stretch mode.

DOI: [10.1103/PhysRevB.79.035423](https://doi.org/10.1103/PhysRevB.79.035423)

PACS number(s): 68.37.Ef, 68.43.Bc, 68.35.Ja

I. INTRODUCTION

Quantum tunneling of hydrogen atoms (or protons) plays crucial roles in diverse chemical, physical, and biological processes.¹⁻⁵ The fundamental aspects of tunneling dynamics have been argued by spectroscopic studies for prototypical molecules such as ammonia and tropolone.⁶⁻⁸ The molecular inversion or proton transfer proceeds via tunneling, which was manifested as spectral doublets in the rotational and vibrational spectra. The tunneling dynamics was found to couple with specific vibrational displacements that reduce effective tunneling barrier and/or path length.

The real-space observation of hydrogen-atom dynamics has been performed by using scanning tunneling microscopy (STM). Quantum tunneling was visualized in the diffusion process of hydrogen atom over Cu(100).⁹ A naphthalocyanine molecule adsorbed on an insulating film was induced and imaged to exchange the two hydrogen atoms between the two equivalent positions in the central cavity of the molecule.¹⁰ The interchange tunneling of the hydrogen-bond donor and acceptor molecules was recently observed in water dimers.¹¹ The interchange motion involves not only hydrogen-bond rearrangement but also substantial displacements of oxygen atoms, which should require multidimensional treatment of the potential-energy surface for quantitative description of the dynamics.

In this work, the dynamics of hydrogen atom in a hydroxyl group and its dimer adsorbed on Cu(110) is studied by using STM and first-principles calculations. The inclined OH axis of the hydroxyl group switches back and forth between the two equivalent orientations. The calculation revealed that the switch motion proceeds via hydrogen-atom tunneling. The motion is enhanced upon the excitation of molecular vibrational mode that manifested itself in the inelastic electron-tunneling spectra (IETS) as peaks or dips, depending on the position of the tip over the molecule. On the other hand, the switch motion is quenched by hydrogen bonding in a hydroxyl dimer.

II. METHODS

The experiments were carried out in an ultrahigh vacuum chamber equipped with STM operating at 6 K.¹¹ An electrochemically etched tungsten tip was used as an STM probe. The STM images were acquired in constant current mode. A single crystalline Cu(110) was cleaned by repeated cycles of argon-ion sputtering and annealing. The clean Cu(110) surface was exposed to H₂O or D₂O gases at 12 K to yield very low coverage, where water molecules exist mainly as isolated monomers. A hydroxyl species was produced by dissociating a water molecule with the STM. A hydroxyl dimer was produced by dragging a water molecule to a preadsorbed oxygen atom by using STM, resulting in the following reaction: H₂O + O → (OH)₂. This reaction was suggested to proceed with a negligible barrier.¹² Actually, the reaction occurs spontaneously when the reactants come close to each other. The preadsorbed oxygen atoms were produced by exposing the surface to molecular oxygen at 40 K. IETS was conducted using a lock-in amplifier with an rms modulation of 6 mV at 590 Hz unless otherwise mentioned. The spectra were recorded repeatedly for accumulation to improve signal-to-noise ratio.

The calculations were based on density-functional theory^{13,14} (DFT) within the generalized gradient approximation (GGA).¹⁵ We used a computer program STATE.¹⁶ The wave functions and the charge density were expanded in terms of plane waves up to the cutoff energies of 25 and 225 Ry, respectively. The electron-ion interaction was described by the pseudopotentials.^{17,18} We used a three-layer Cu slab, unless otherwise mentioned, with surface OH monomer (dimer) on one side of the slab arrayed in a 2 × 3 (3 × 3) surface unit cell, and the vacuum region of 12.89 Å was inserted between slabs. A GGA-optimized lattice constant of 3.64 Å, which is 0.8% larger than the experimental value of 3.61 Å, was used to construct the slabs. A (4 × 4) Monkhorst-Pack¹⁹ *k*-point set was used to sample the surface

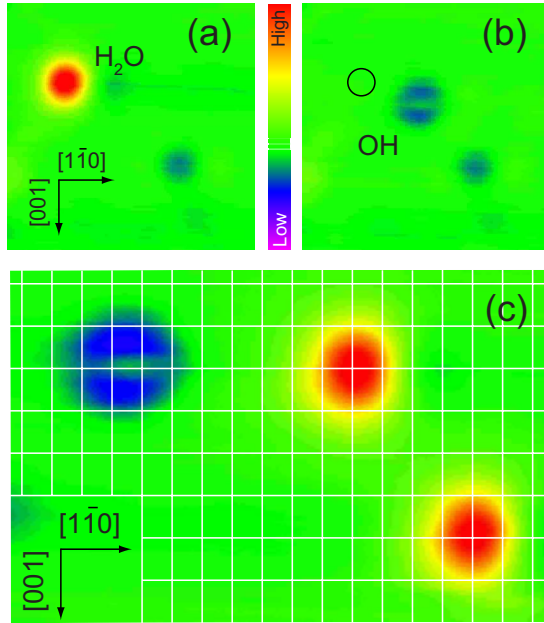


FIG. 1. (Color online) (a) A voltage pulse of 2 V for 0.5 s was applied to a water molecule imaged as a round protrusion. The tip height during the pulse was fixed vertically to yield 0.5 nA tunneling current at 24 mV sample bias. (b) The product (OH species) appears as paired depressions. The original position of the water molecule is shown by a circle. The image size is $47 \times 47 \text{ \AA}^2$. (c) The relative position of OH species to nearby water molecules. The grid lines indicate the lattice of the Cu(110) surface, which are drawn in such a way that the water molecules are located on top of Cu atoms. The image size is $46 \times 30 \text{ \AA}^2$. All images were acquired at 24 mV and 0.5 nA.

Brillouin zone, and the Fermi level was treated by the first-order Methfessel-Paxton scheme²⁰ with the 0.05 eV smearing width. During the structural optimization, adsorbates and two topmost Cu layers were allowed to relax until the forces on them were less than 0.05 eV/Å. We verified that the adsorption energy of OH monomer and the energy barrier of its flip-flop motion are less than 0.06 and 0.03 eV, respectively, when we increase the slab thickness up to seven layers. The molecular graphics were produced by the XCRYSDEN graphical package.²¹

III. RESULTS AND DISCUSSION

A. Hydroxyl production

Figure 1 shows the production of a hydroxyl species from a water molecule with the STM. The water molecule appears as a round protrusion with an apparent height of 0.6 Å [Fig. 1(a)]. A voltage pulse of $V_s=2 \text{ V}$ for 0.5 s was applied with the tip positioned over the water molecule. The image after the pulse [Fig. 1(b)] shows that the molecule has reacted into a hydroxyl species imaged as paired depressions (-0.1 \AA) aligned along [001]. A small depression on the right is an unidentified impurity used as a marker. The reaction competes with translation of the parent water molecule, and the product is usually observed away from the original position. The reaction can be induced with a probability of $\sim 50\%$

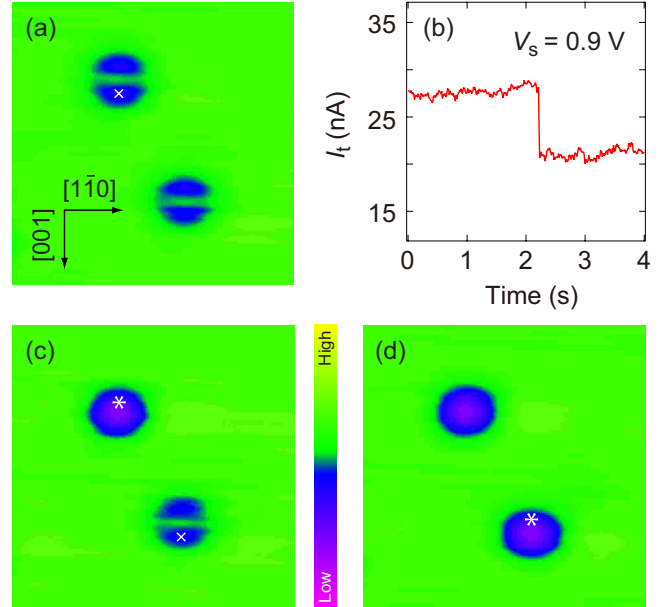


FIG. 2. (Color online) Sequence of STM-induced dissociation of two OH species on Cu(110) ($42 \times 42 \text{ \AA}^2$). (a) A voltage pulse of 0.9 V was applied over the depression (indicated by a cross) of the top left molecule. The tip height during the pulse was fixed vertically to give 0.5 nA at 24 mV. (b) The tunneling current during the voltage pulse. [(c) and (d)] Images taken after the pulses show the successive changes into round depressions which are assigned as atomic oxygen. The short-bridge site occupied by the parent OH is indicated by an asterisk, indicating that the product is displaced along [001] and located at an adjacent hollow site. All images were acquired at 24 mV and 0.5 nA.

with a pulse of 2 V for 0.5 s. Water molecules were found to be located on top of Cu atoms from their relative position to coadsorbed CO molecules,²² which are known to be adsorbed on top of Cu atoms.²³ The DFT calculation by Tang and Chen²⁴ showed that water molecules deviate from the exact top site by 0.88 Å, while Ren and Meng²⁵ predicted relatively slight displacement of 0.5 Å. In our calculation with five-layer Cu slabs, the latter position was most favorable with the adsorption energy of 0.34 eV, while the energy difference between these sites and the top site was within 20 meV. This may reflect the general property of water-metal interaction that the potential-energy surface is smooth along the surface in the vicinity of the top site,²⁶ so that the molecule is delocalized around the top site. Accordingly, the position of the product is determined from its relative location to nearby water molecules to be short-bridge site [Fig. 1(c)], in agreement with the theoretical predictions.^{12,25,27}

The assignment of the paired depression to a hydroxyl species was confirmed by further dissociating it into atomic oxygen. Figure 2(a) shows two OH species produced from two water molecules. The tip was positioned over the depression (indicated by a cross) and a 0.9 V pulse was applied. The current during the voltage pulse [Fig. 2(b)] shows an abrupt drop, indicating the moment of the reaction. The image after the pulse [Fig. 2(c)] shows that it has been dissociated into atomic oxygen imaged as a round depression with an apparent height of -0.3 \AA . The asterisk indicates the

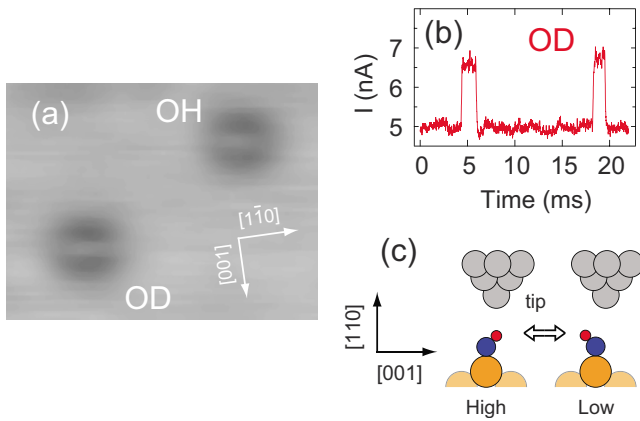


FIG. 3. (Color online) (a) STM images for OH and OD species on Cu(110) obtained at 24 mV and 5 nA. The image size is $40 \times 30 \text{ \AA}^2$. (b) Tunneling current with the tip fixed over the depression of OD at the height corresponding to 24 mV and 5 nA. The sample voltage was 24 mV during the measurement. (c) Schematic of OD switching between the two orientations under the tip.

original position of the parent OH species (short-bridge site). Thus the product is displaced and located on the adjacent hollow site, in agreement with the previous result which used molecular oxygen to produce atomic oxygen.²⁸ Another OH species was successively dissociated [Fig. 2(d)]. The product was always observed at one of the adjacent hollow sites depending on the position of the pulse injection. Thus the hydroxyl dissociation was better controlled than the production. The reaction was observed at both bias polarities, and the thresholds were 0.9(1.5) V for OH(OD) with the variation of ~ 0.2 V between the tip conditions.²⁹ The dissociation is presumably induced via multiple vibrational excitation of internal stretch by tunneling electrons. The isotope effect can be ascribed to the reduced lifetime of the vibrational excited states, since the lower vibrational energy of O-D stretch causes a more efficient decay of the excited state that hinders the vibrational up-pumping process.³⁰

B. Dynamics of a hydroxyl species

A remarkable isotope effect was observed for the dynamical properties of the hydroxyl species. The dynamical behavior of OD is observed as two-state fluctuation in the tunneling current recorded with the tip fixed over the depression [Fig. 3(b)], while no such fluctuation was observed for OH. Thus we can discriminate between the two isotopomers, although they are rather difficult to be discerned in the image [Fig. 3(a)]. The previous calculations^{12,25,27} and experiment³¹ showed that the OH axis is inclined along [001]. We have theoretically confirmed the inclined geometry [Fig. 4(a)], where the geometrical parameters are almost the same as those reported previously.¹² To understand the dynamical behavior, we calculated the potential-energy surface of OH along the lateral coordinates of hydrogen atom [Fig. 4(b)]. The positions of oxygen atom and the top two-layer Cu atoms were optimized at each point. The two minima correspond to the inclined geometries, and the molecule can switch the orientation via the transition state of upright ge-

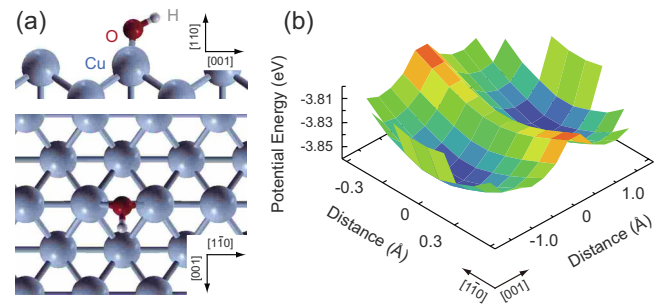


FIG. 4. (Color online) (a) Side (upper) and top (lower) views of the calculated structure for adsorbed OH. The OH bond length and the angle between the axis and the surface normal are 0.99 \AA and 62° , respectively. (b) Calculated potential-energy surface of OH as a function of the lateral displacements of hydrogen atom from the top of the bridge site. The two minima correspond to the inclined geometries, and the potential barrier between the minimum and the saddle point (for switch motion) is 0.14 eV. The potential minima are 3.94 eV in depth with respect to free OH.

ometry. Although the potential barrier for switching ($V_B = 0.14$ eV) is too high to be overcome by thermal activation at 6 K, the molecule may flip via hydrogen-atom tunneling. The tunneling rate was roughly estimated by WKB approximation,

$$R = \nu \exp \left\{ -\frac{2}{\hbar} \int_{-d/2}^{d/2} \sqrt{2m[V(x) - V_0]} dx \right\}, \quad (1)$$

where ν , d , m , and V_0 are vibrational frequency, tunneling path length, mass of hydrogen atom, and zero-point energy, respectively. $V(x)$ is the potential curve approximated by a quartic function. Using the calculated parameters,³² the tunneling rates were estimated to be $10^{6(2)} \text{ s}^{-1}$ for OH (OD). Thus we suggest that the paired depressions in the STM image result from the fast flip-flop tunneling of the inclined hydroxyl groups. The observed isotope effect is ascribed to the difference in the tunneling rates; OH flips much faster than OD, and the associated fluctuation is smeared out for OH due to the limited bandwidth of the preamplifier.

The high-current (low-current) states are tentatively assigned to the orientations of OD pointing toward (away from) the tip [Fig. 3(c)]. The STM simulation based on the Tersoff-Hamann approach³³ suggests that the side of hydrogen atom appears brighter than the opposite position. We note that the low-current state is more preferred in Fig. 3(b), suggesting that there exists substantial tip-surface interaction that stabilizes the low-current state. Indeed, at lower current with larger tip-surface distance, the preference was observed to attenuate; the fractional occupation of the high-current state was 0.04 ± 0.02 at 24 mV and 5 nA, and increases to 0.15 ± 0.03 as the tip is retracted and the tunneling current decreases to 0.05 nA. Under the condition of Fig. 3(b), the switch rate of OD from the low to high states is estimated to be $(0.9 \pm 0.4) \times 10^3 \text{ s}^{-1}$. The values depend on the tip condition within the variation.

The d^2I/dV^2 spectra (IETS) for OD [Fig. 5(a)] and OH [Fig. 5(b)] exhibit peaks (dips) at 41 (−45) and 58 (−62) mV at positive (negative) sample bias, respectively.

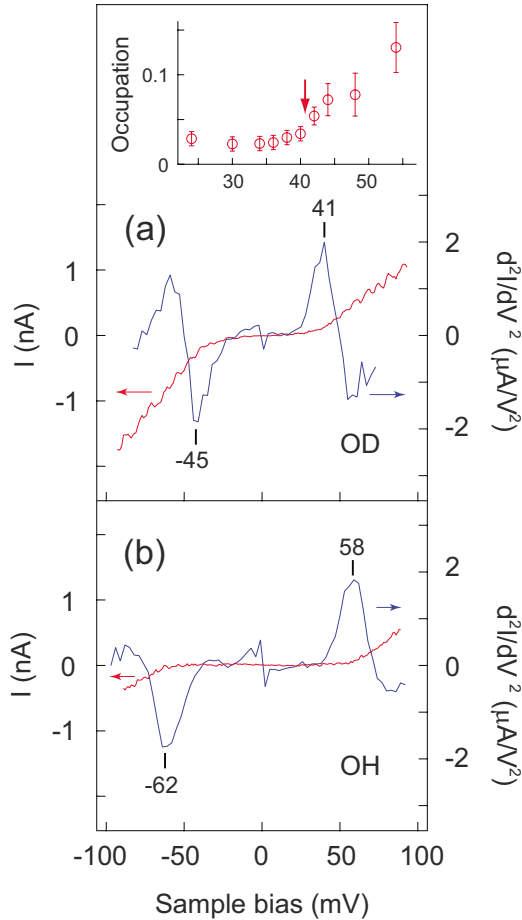


FIG. 5. (Color online) (a) The background-subtracted I - V and d^2I/dV^2 spectra (IETS) measured over the depression of OD. The inset shows fractional occupation of the high-current state for OD measured as a function of bias voltage. The tip height was fixed at 24 mV and 5 nA in both cases. (b) The same as (a) but acquired for OH. The I - V curves are average of 300 and 200 scans for OD and OH, respectively.

The I - V curves show abrupt increase or decrease at these voltages. Both the d^2I/dV^2 and I - V curves are displayed after subtraction with those measured over the clean surface. The peak (dip) voltage was not dependent on the tip-surface distance, corresponding to the set point from 0.05 to 5 nA at 24 mV. Hereafter we focus on the positive bias. The two-state fluctuation of OD [Fig. 3(b)] was investigated as a function of the bias voltage, and the fractional occupation of the high-current state is shown in the inset of Fig. 5(a). The switch motion is enhanced and the fractional occupation increases abruptly at the onset voltage that coincides with the peak in the IETS (arrow). This suggests that the IETS peak arises from the electron-induced enhancement of the switch motion.³⁴ The peak voltage shows an isotope effect of 1.4, suggesting that the switch motion is induced by inelastic excitation of OH(OD) bending modes. The vibrational energies are in good agreement with the values estimated above from the potential curvature.³² Also the previous calculation predicted a vibration peak at ~ 60 meV for OH.²⁷ This mode is directly along the reaction (switch) coordinate. Therefore, the vibrational excitation assists the tunneling, in analogy

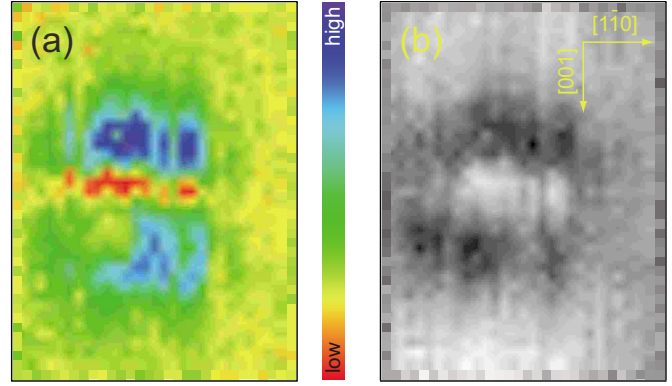


FIG. 6. (Color online) (a) Spatial map of the IETS intensity for OH. At each pixel, the feedback was disabled at the tip height to give 5 nA at 24 mV, and the vibrational intensity was acquired at 54 mV with the bias modulation of 12 mV_{rms}. The IETS intensity ranges from -0.5 to $1.6 \mu\text{A}/\text{V}^2$ with respect to the background. (b) Simultaneously acquired topographic image at 24 mV and 5 nA. The image size is $11 \times 14 \text{ \AA}^2$.

with the inversion tunneling of ammonia that is efficiently coupled with the umbrella mode.⁶ It is noted that, in the IETS, the peaks are accompanied with a dip at their higher-voltage side. This is ascribed to the saturation of the fractional occupation, as will be described later in detail.

The spatial distribution of the IETS peak intensity and simultaneously acquired topographic image are shown in Figs. 6(a) and 6(b), respectively. The vibrational intensity is highest over the depressions in the topography. A remarkable feature is that the negative vibrational intensity, i.e., the decrease in the differential conductance, occurs when the tip is positioned over the center between the two depressions. As the switch motion is enhanced by tunneling electron, the mean distribution of hydrogen atom increases around the transition region, which may temporally perturb the electronic structure and thus result in the decrease in the conductance around the center. Since the region of the negative intensity is fairly narrow along the [001] direction ($\sim 1.5 \text{ \AA}$), it was observed only with a sharp tip. The IETS has exhibited either peak or dip structure for various adsorbate systems,³⁵ depending on the coupling of the vibrational mode with the electronic structure in the junction.³⁶ In the present case, both the peak and dip appear depending on the lateral position of the tip over the same molecule. We propose that this is a general phenomenon that appears when molecular motion is involved in the inelastic tunneling process.

C. Hydroxyl dimer

The molecular interaction has a marked impact on the dynamical property of the hydroxyl group. When dimerized, it is imaged as either of the two equivalent tautomers [Figs. 7(a)–7(c)], indicating that the switch motion is quenched. The structure of the dimer was calculated and it is found to be substantially stabilized (0.22 eV compared to two isolated hydroxyls) by hydrogen bonding [Fig. 7(d)], which is the origin of the quenching. The two hydroxyl groups, bonded to

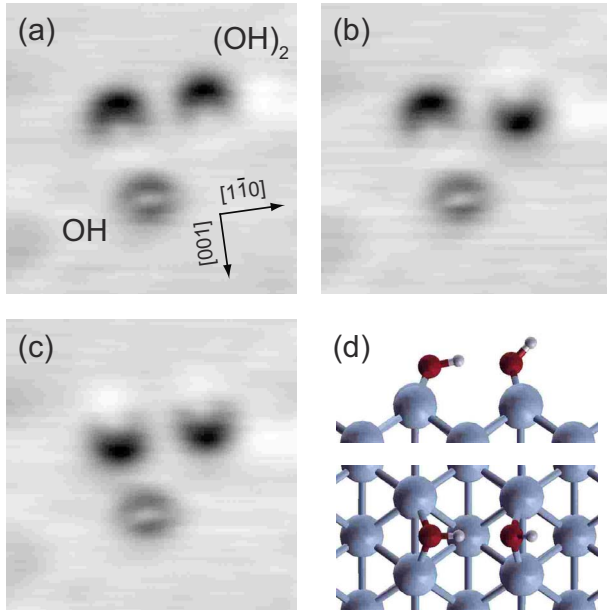


FIG. 7. (Color online) (a) Topographic images of two OH dimers compared with an OH monomer. (b) One of the dimers was flipped by a 0.4 V pulse. (c) Another is also flipped in the same way. The images were obtained at 24 mV and 5 nA, and the size is $35 \times 35 \text{ \AA}^2$. (d) Side (upper) and top (lower) views of the calculated structure for the OH dimer. The hydrogen-bond OH-O distance is 1.83 Å. The OH bond length and the tilt angles to the surface normal for the H-bond donor (acceptor) are 1.00(0.98) Å and 78.6° (43.4°), respectively.

the adjacent bridge sites along [001], are displaced and re-oriented to take the optimal configuration for hydrogen bonding. The quenching of the OH switch was proposed to occur due to adjacent H impurity as well.²⁵ Indeed, the H atom, although invisible with the STM, should be present on the surface as a result of the OH production from water and might affect the switch motion of the hydroxyls. The hydroxyl monomer was always observed as paired depressions (not quenched) as far as it was isolated from impurities, suggesting that the H atom is not present in the vicinity of the hydroxyl species. The produced H atom may diffuse away due to its small diffusion barrier along the trough.^{12,37} The hydroxyls in the dimer may switch their orientations via tunneling in a concerted manner. The tunneling rate is roughly estimated with double mass and the barrier height [$V_B \approx (0.14 \times 2 + 0.22) \text{ eV}$] is $\sim 10^{-11} \text{ s}^{-1}$ from Eq. (1), corroborating that the tunneling is almost quenched for the hydroxyl dimer.

Although the intrinsic motion is quenched, the dimers are induced to flip by tunneling electron, which results in the two-state fluctuation of the tunneling current under high bias voltage [Fig. 8(a)] and consequently gives a nonlinear feature in the averaged I - V curve [solid curve in Fig. 8(b)]. The tip was fixed over the depression of $(\text{OD})_2$ at the height corresponding to 24 mV and 0.05 nA. The tunneling current at the high and low states, together with their fractional occupation, were obtained as a function of the voltage [Fig. 8(c)]. Using these data, the averaged I - V curve is well reproduced in a similar way as described in Ref. 34 [circles in Fig.

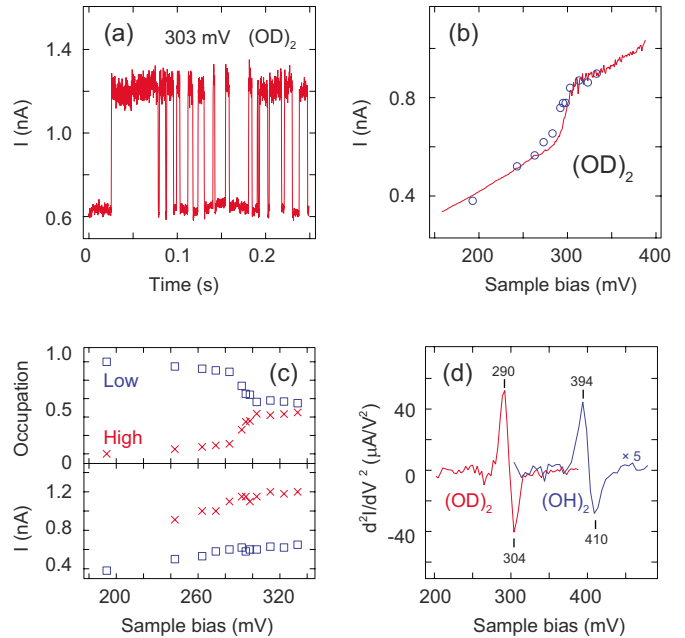


FIG. 8. (Color online) (a) Temporal evolution of tunneling current over $(\text{OD})_2$ during the pulse voltage of 303 mV. The tip was fixed over the depression at the set point of 0.05 nA and 24 mV, and then the feedback was turned off and the voltage was applied. (b) Averaged I - V curve of 60 scans obtained over the depression of $(\text{OD})_2$ at the set point of 0.05 nA and 24 mV (solid curve). (c) The state-resolved I - V plots (lower panel) and the relative occupation (upper panel) for the low (squares) and high (crosses) states as a function of the bias voltage for $(\text{OD})_2$. These data were obtained at the same height as (b) and used to reproduce the averaged I - V curve (circles) in (b). (d) The IETS spectra for $(\text{OD})_2$ and $(\text{OH})_2$. The peak and dip voltages in the IETS were determined by fitting the spectra to the derivative of a Gaussian function. The spectra were obtained over the depressions at the set points of 0.5 and 5 nA at 24 mV for $(\text{OH})_2$ and $(\text{OD})_2$, respectively. The $(\text{OH})_2$ would be broken during the measurement with the set point of 5 nA.

8(b)]. The nonlinear feature is ascribed to the abrupt changes in the fractional occupation, and its onset voltage is determined to be 290 mV from the peak in the IETS [Fig. 8(d)]. This peak is accompanied with a dip at 304 mV, which is now clearly ascribed to the saturation of the fractional occupation. The peak position shifts to 394 mV for $(\text{OH})_2$. The peak voltage and the isotope shift suggest that the motion is induced by O-H(O-D) stretch excitation. The vibrational energy is significantly redshifted from that for free OH [443 meV for OH (Ref. 38)], bearing the evidence for hydrogen-bonding interaction in the dimer. For hydrogen-bonded OH groups on Pd(100), the O-H stretch mode was observed at 403 mV.³⁹ While the rupture of hydrogen bond requires 0.22 eV, it may be induced by the excitation of the O-H stretch mode, eventually leading to the switching of the dimer.

IV. SUMMARY

A hydroxyl species is inclined on Cu(110) and switches the orientation via tunneling. The switch motion is enhanced upon the excitation of the bending mode that directly corre-

lates with the reaction coordinate. The enhanced motion gives rise to a peak or a dip in IETS, depending on the position of the tip over the molecule. The switch motion is quenched by hydrogen bonding in a hydroxyl dimer and is induced by the excitation of hydrogen-bonded O-H stretch mode.

ACKNOWLEDGMENTS

The authors thank the Supercomputer Center, Institute for Solid State Physics, University of Tokyo for the use of the facilities. H.O. acknowledges valuable discussion with Koji Ando.

*hokuyama@kuchem.kyoto-u.ac.jp

- ¹R. P. Bell, *The Tunnel Effect in Chemistry* (Chapman and Hall, London, 1980).
- ²K. W. Kehr, in *Hydrogen in Metals I and II*, edited by G. Alefeld and J. Völkl (Springer, Berlin, 1978).
- ³Y. Moritomo, Y. Tokura, N. Nagaosa, T. Suzuki, and K. Kumagai, *Phys. Rev. Lett.* **71**, 2833 (1993).
- ⁴J. M. J. Swanson, C. M. Maupin, H. Chen, M. K. Petersen, J. Xu, Y. Wu, and G. A. Voth, *J. Phys. Chem. B* **111**, 4300 (2007).
- ⁵A. Kohen, R. Cannio, S. Bartolucci, and J. P. Klinman, *Nature (London)* **399**, 496 (1999).
- ⁶G. Herzberg, *Molecular Spectra and Molecular Structure II, Infrared and Raman Spectra of Polyatomic Molecules* (Van Nostrand, Princeton, 1945).
- ⁷K. Tanaka, H. Honjo, T. Tanaka, H. Kohguchi, Y. Ohshima, and Y. Endo, *J. Chem. Phys.* **110**, 1969 (1999).
- ⁸R. L. Redington and R. L. Sams, *J. Phys. Chem. A* **106**, 7494 (2002).
- ⁹L. J. Lauhon and W. Ho, *Phys. Rev. Lett.* **85**, 4566 (2000).
- ¹⁰P. Liljeroth, J. Repp, and G. Meyer, *Science* **317**, 1203 (2007).
- ¹¹T. Kumagai, M. Kaizu, S. Hatta, H. Okuyama, T. Aruga, I. Hamada, and Y. Morikawa, *Phys. Rev. Lett.* **100**, 166101 (2008).
- ¹²Q.-L. Tang and Z.-X. Chen, *J. Chem. Phys.* **127**, 104707 (2007).
- ¹³P. Hohenberg and W. Kohn, *Phys. Rev.* **136**, B864 (1964).
- ¹⁴W. Kohn and L. J. Sham, *Phys. Rev.* **140**, A1133 (1965).
- ¹⁵J. P. Perdew, K. Burke, and M. Ernzerhof, *Phys. Rev. Lett.* **77**, 3865 (1996).
- ¹⁶Y. Morikawa, *Phys. Rev. B* **51**, 14802 (1995).
- ¹⁷N. Troullier and J. L. Martins, *Phys. Rev. B* **43**, 1993 (1991).
- ¹⁸D. Vanderbilt, *Phys. Rev. B* **41**, 7892 (1990).
- ¹⁹H. J. Monkhorst and J. D. Pack, *Phys. Rev. B* **13**, 5188 (1976).
- ²⁰M. Methfessel and A. T. Paxton, *Phys. Rev. B* **40**, 3616 (1989).
- ²¹A. Kokalj, *Comput. Mater. Sci.* **28**, 155 (2003); code available at <http://www.xcrysden.org/>
- ²²T. Kumagai, S. Kaizu, H. Okuyama, S. Hatta, T. Aruga, I. Hamada, and Y. Morikawa, *e-J. Surf. Sci. Nanotechnol.* **6**, 296 (2008).
- ²³M. Doering, J. Buisset, H.-P. Rust, B. G. Briner, and A. M. Bradshaw, *Faraday Discuss.* **105**, 163 (1996).
- ²⁴Q.-L. Tang and Z.-X. Chen, *Surf. Sci.* **601**, 954 (2007).
- ²⁵J. Ren and S. Meng, *Phys. Rev. B* **77**, 054110 (2008).
- ²⁶A. Michaelides, V. A. Ranea, P. L. de Andres, and D. A. King, *Phys. Rev. Lett.* **90**, 216102 (2003).
- ²⁷J. Ren and S. Meng, *J. Am. Chem. Soc.* **128**, 9282 (2006).
- ²⁸B. G. Briner, M. Doering, H.-P. Rust, and A. M. Bradshaw, *Phys. Rev. Lett.* **78**, 1516 (1997).
- ²⁹The thresholds for the dissociation were determined as follows. The tip was fixed over one of the depressions of an OH(OD) species at the height that yields 0.5 nA at 24 mV, and then a voltage pulse was applied. We defined the threshold as the minimum voltage that induces a reaction within 10 s.
- ³⁰Ph. Avouris, R. E. Walkup, A. R. Rossi, H. C. Akpati, P. Nordlander, T.-C. Shen, G. C. Abeln, and J. W. Lyding, *Surf. Sci.* **363**, 368 (1996).
- ³¹M. Polak, *Surf. Sci.* **321**, 249 (1994).
- ³² $h\nu$ ($=2V_0$) was estimated to be 64(45) meV for OH(OD) by harmonic approximation of the local minima along [001]. The motion except for hydrogen atom was neglected, and it was assumed to move circularly between the inclined geometries ($\pm 62^\circ$ from the surface normal) with the O-H bond length fixed (0.99 Å). Accordingly, the path length d is 2.1 Å.
- ³³J. Tersoff and D. R. Hamann, *Phys. Rev. Lett.* **50**, 1998 (1983).
- ³⁴J. Gaudioso, L. J. Lauhon, and W. Ho, *Phys. Rev. Lett.* **85**, 1918 (2000).
- ³⁵W. Ho, *J. Chem. Phys.* **117**, 11033 (2002).
- ³⁶H. Ueba, T. Mii, and S. G. Tikhodeev, *Surf. Sci.* **601**, 5220 (2007).
- ³⁷M. Nishijima, H. Okuyama, N. Takagi, T. Aruga, and W. Brenig, *Surf. Sci. Rep.* **57**, 113 (2005).
- ³⁸G. Herzberg, *Molecular Spectra and Molecular Structure I, Spectra of Diatomic Molecules* (Van Nostrand, Princeton, 1950).
- ³⁹M. Stuve, S. W. Jorgensen, and R. J. Madix, *Surf. Sci.* **146**, 179 (1984).